Dynamical and scaling effects in two-dimensional superfluid helium

R. Brada,* H. Chayet, and W. I. Glaberson
Racah Institute of Physics and Astronomy, The Hebrew University, Givat-Ram, Jerusalem, Israel
(Received 7 December 1992; revised manuscript received 23 April 1993)

The results of a series of measurements of Kosterlitz-Thouless behavior in helium films are presented. Use is made of high-Q piezoelectric crystals so as to probe the phenomena in a single flat substrate geometry at high frequencies. Variations of the superfluid density and dissipation in the vicinity of the transition were measured. Dynamical effects were probed by comparing transitions at two different frequencies. Results are compared with a comprehensive numerical calculation in which finite-size scaling effects are explicitly introduced. A consistent picture for the dependence of critical thickness on temperature, of the scaling of the transition shape with temperature, and of dynamical effects is obtained.

I. INTRODUCTION

In recent years there has been a great deal of interest in two-dimensional (2D) superconducting and superfluid helium systems. In these systems, thermally activated vortex-antivortex pairs are the dominant fluctuations and mediate the transition from the respective superfluid and superconducting phases. The static theory of these 2D phase transitions, which fall in the same universality class as the XY (Ref. 1) model, has been very successful. The theory, developed by Kosterlitz and Thouless,[2] associates the transition from the superfluid to the normal phase with the unbinding of thermally activated vortex-antivortex pairs at the static transition temperature T_{KT}. The unbinding is a cooperative effect which destroys the algebraic long-range order of the system at some nonzero superfluid density proportional to the transition temperature.[3]

Kosterlitz and Thouless used renormalization-group techniques to solve the problem of a dilute gas of logarithmically interacting vortex-antivortex pairs. By considering the effects of smaller pairs on the interaction between the members of larger pairs, they were able to extract a scale-dependent dielectric constant and vortex-pair excitation probability. The scale dependence of these parameters is given by the Kosterlitz-Thouless recursion relations. For an experiment carried out at zero frequency, the recursion relations are iterated to infinite scale. The transition temperature is defined as the highest temperature for which the vortex-pair excitation probability no longer vanishes at infinite scale, i.e., infinite pair separation.

To interpret experiments at finite frequencies, the Kosterlitz-Thouless static theory must be incorporated into a more comprehensive theory which accounts for the dynamic response of the vortex plasma to an oscillating field. Ambegaokar *et al.*[4] and Ambegaokar and Teitel[5] have shown that the vortex diffusion length r_D is the characteristic separation beyond which pairs can no longer equilibrate to the external field. This leads to two modifications of the static theory.[2] First, because pairs larger than r_D do not participate in the renormalization, the Kosterlitz-Thouless recursion relations are not to be iterated out to infinite scale but to a finite cutoff. This, in effect, shifts the transition temperature up from T_{KT} to a new frequency-dependent dynamic transition temperature T_c and produces rounding of the transition. Second, the effective dielectric constant becomes complex, the imaginary part being associated with dissipative vortex motion.

In all the above discussion, the principal assumption is made that the film is indeed two dimensional. Under what circumstances this assumption is justified in experiments on thin layers of helium is not completely clear, but it is generally believed that whenever the three-dimensional correlation length is not much smaller than the thickness of the film, Kosterlitz-Thouless behavior pertains. This hypothesis is somewhat complicated by the fact that bulk three-dimensional behavior is expected to be significantly modified by finite-size effects, under these circumstances, without regard to the two dimensionality of the system. For example, one would expect a significant decrease in the average superfluid density, associated with healing of the order parameter at the system boundaries, even in the absence of vortex-antivortex excitations. We find that in the vicinity of all superfluid transitions in helium films, finite-size effects dominate the bare, unrenormalized, behavior, while the actual transition behavior is determined by the Kosterlitz-Thouless mechanism. It may very well be that at temperatures sufficiently below the Kosterlitz-Thouless transition, finite-size effects alone are important. The reader is referred to a comprehensive review of finite-size scaling effects by Gasparini.[6]

It is the purpose of this paper to describe a series of measurements of phase-transition behavior—both superfluid density and dissipation—in helium films whose thicknesses vary from 12.8 to 63 Å and whose transition temperatures range from 1.38 to 2.1 K. Use is made of a high-Q quartz microbalance, thereby avoiding capillary condensation effects present in mylar roll or stack geometries. We find reasonable agreement between our measured values of transition temperature and shape and the results of a simple theoretical calculation in which finite-size scaling is used to determine the background superfluid density which is then used as the start-

0163-1829/93/48(17)/12874(12)/$06.00

ing point for Kosterlitz-Thouless renormalization. Measurements at different frequencies yield shifts of transition thickness consistent with predictions of the dynamical theory.

II. PREVIOUS EXPERIMENTS AND THEORETICAL BACKGROUND

A. 2D superfluidity

Superfluid flow in thin films, observed in 1940 by Long and Meyer,[7] suggested that 2D superfluidity can be realized, in spite of rigorous theoretical proofs[8] that the superfluid order parameter is destroyed in two or fewer dimensions. Other experiments followed supporting their conclusion: Bowers, Brewer, and Mendelssohn[9] measured the heat transfer in unsaturated films in 1951 and found that the mobility of a thin film decreases rapidly as the temperature is raised, and above some critical temperature no film transfer occurs. In another heat-transfer experiment Long and Meyer[10] confirmed the existence of the so-called "onset temperature," lower than the bulk critical temperature, where the film becomes superfluid. Critical flow rate experiments to determine T_c as a function of film thickness were performed by Brewer and Mendelssohn[11] in 1961. In 1969 Henkel, Smith, and Reppy[12] demonstrated that the angular momentum associated with a persistent current is linearly related to the film thickness, provided that the film thickness is greater than some critical value depending on temperature. This critical value was deduced from the linear extrapolation to the point of zero mass flow. Propagation of temperature waves in thin films of helium performed by Everitt, Atkins, and Denenstein[13] and later by Rudnick *et al.*[14] provided additional evidence of superfluid behavior, but a clear superfluid transition in third-sound measurements was reported only later by Rudnick[15] in 1978. Data obtained in this experiment confirmed the universal jump in superfluid areal density predicted by Kosterlitz-Thouless theory.

In all the measurements above, in order to determine the transition to the superfluid state, one has to establish mass flow by means of pressure or temperature gradients. However, these measurements cannot be employed to examine the superfluid density continuously through the transition region, since the persistent currents decay away and third sound becomes heavily damped and ceases to propagate. To overcome these difficulties, an ac microbalance technique was introduced for 2D helium studies. Here one measures only the normal component of the fluid which is viscously clamped to the oscillating substrate. In an adaptation of Andronikashvili's[16] torsional-oscillator technique, Bishop and Reppy[17] (1978) had been able to provide a quantitative characterization of the superfluid transition. In the original Andronikashvili oscillator, a stack of closely spaced annular disks at the end of a torsional fiber was placed in a bath of superfluid helium. The plates were closely spaced so that the normal fluid is clamped to them and dragged along as they oscillate, while the superfluid is not seriously affected. By measuring the resonant frequency of the system one can determine the superfluid density of the liquid. Bishop and Reppy's device consisted of an extremely high-Q torsional oscillator ($Q > 10^5$) using a rolled layered Mylar substrate. More detailed measurements for thin-film coverage, corresponding to transition temperatures in the range of 70 mK–0.5 K, were reported by Agnolet, McQueeney, and Reppy[18] in 1989, and they confirmed some of the essential features of the Kosterlitz-Thouless theory.

In a recent work, Shirahama, Kubota, and Ogawa[19] used a torsional oscillator method for the study of the nature of the transition for films adsorbed on porous glasses. The situation is significantly complicated because of the 3D global structure of the porous substrate. Effects presumably associated with limitations on vortex-pair interactions owing to finite pore sizes were observed. To determine the effects of frequency on the transition temperature, the measurements were performed with two oscillators having different resonant frequencies. An increase of the transition temperature associated with increased frequency was observed. Because of the complicated geometry used in these experiments, it is difficult to make a direct comparison with results reported here.

Another microbalance technique involves the use of a quartz crystal as a single oscillating substrate. For measurements in thin films of helium this technique was used by Chester, Yang, and Stephens in 1972,[20] and was later used for more quantitative measurements of the superfluid fraction by Chester and Yang[21] and Herb and Dash.[22] Unlike the torsional oscillator technique of Bishop and Reppy, these experiments were performed at relatively high frequencies and showed a considerable broadening of the transition region.

B. Theory

Our approach to a theoretical understanding of our data involves an attempt to integrate several different, but possibly intimately related, notions. It is obvious from the shape of the transition that Kosterlitz-Thouless renormalization plays a vital role in the phenomenology. On the other hand, a straightforward iteration of the KT recursion relations from any reasonable starting conditions yields a critical film thickness much smaller—typically a factor of 3 smaller—than that observed. It quickly becomes obvious that significant Kosterlitz-Thouless renormalization of the superfluid density occurs only where the film thickness is not much larger than the three-dimensional coherence length. In this regime, the superfluid density has already been significantly suppressed by finite-size scaling effects. A concrete expression of finite-size scaling that we choose to use is the Ψ theory of Ginzburg and co-workers.[23,24] In this approach, the superfluid density is pulled to zero at the film boundaries, recovering to its bulk value in a characteristic healing scale equal to the temperature-dependent three-dimensional coherence length. Yet another issue involves a possible "dead layer" between the superfluid and substrate. The van der Waals interaction responsible for the adsorption of the film on the substrate gives rise

to a strong pressure gradient near the substrate. Using the bulk phase diagram would suggest that the superfluidity is suppressed by hydrostatic pressure out to a distance of the order of two atomic layers.[25] This last effect is relatively unimportant for thick films, but cannot be ignored otherwise. Film excitations such as ripplons are presumably important for very thin films, but are ignored in this analysis.

We must contend with a number of questions that involve the inter-relation of these various effects. To what extent does crossover to two dimensionality impose Kosterlitz-Thouless behavior in place of finite-size scaling and to what extent does it merely supplement? Is it obvious that the superfluid density is pulled to zero at the free film surface as well as at the substrate?[26] Can one take the bulk phase diagram seriously on an atomic scale or does healing behavior in fact take place within the dead layer? Precise answers to these questions will not be forthcoming but we do suggest an approach that we believe to be reasonable and which, at the same time, yields results reasonably consistent with our experimental data.

Our basic suggestion is that finite-size scaling prepares the background state from which Kosterlitz-Thouless renormalization operates. That is, the bare vortex-antivortex interaction is determined by an areal superfluid density which already incorporates healing length effects. This would be the measured superfluid density, for example, in a situation where vortex-induced screening were somehow totally suppressed. We leave, for the present, the question of the role of the dead layer.

Following Ginzburg and Sobyanin,[23] we introduce a macroscopic wave function

$$\Psi(r,t)=\eta(r,t)e^{i\varphi(r,t)}, \quad \eta\equiv|\Psi| \ . \tag{2.1}$$

The phase of this function is related to the superfluid velocity by

$$v_s=(\hbar/m)\nabla\varphi \ , \tag{2.2}$$

where m is the mass of a helium atom, and the modulus of Ψ is related to the superfluid mass density

$$\rho_s=m|\Psi|^2=m\eta^2 \ . \tag{2.3}$$

For helium at rest, but in a situation where spatial variations of Ψ are possible, Ginzburg and Sobyanin obtain

$$\nabla_*^2\left[\frac{\Psi}{\Psi_0}\right]=\frac{3}{3+M}\left[-\varepsilon^{4/3}+(1-M)\varepsilon^{2/3}\left[\frac{\Psi}{\Psi_0}\right]^2+M\left[\frac{\Psi}{\Psi_0}\right]^4\right]\left[\frac{\Psi}{\Psi_0}\right] \ , \tag{2.4}$$

where $\varepsilon=|T_\lambda-T|$, $\Psi_0=(k\rho_\lambda/mT_\lambda^{2/3})^{1/2}$, T_λ is the three-dimensional transition temperature, and ρ_λ is the fluid density at T_λ. The reduced variable with respect to which the spatial derivatives are taken is normalized as follows:

$$r_*=r\Big/\left[\frac{\hbar^2kT_\lambda^{1/3}}{2m^2\Delta C_p}\right]^{1/2} \ , \tag{2.5}$$

where ΔC_p is the jump in the specific heat from the branch $T<T_\lambda$ to the branch $T>T_\lambda$. The various powers of ε which appear come from the assumed power-law behavior of the bulk superfluid density, $\rho_s/\rho_\lambda=k\varepsilon^{2/3}$.

It is clear that if the wave function is required to vanish at the boundaries, then the average superfluid density is suppressed by an amount that depends on d/l_h where d is the film thickness, l_h is a temperature-dependent healing length diverging as $\varepsilon^{-2/3}$ and M is a parameter that determines the relative strength of the $|\Psi|^6$ term in the expansion of the Gibbs free energy. In what follows, we take the value of M to be 2. We use this approach to determine the bare areal superfluid density in the film, σ_s^0, which in turn is used to determine one of the starting conditions for Kosterlitz-Thouless renormalization. The end result of these considerations is to reduce σ_s^0 from that of a "bulk" layer of the same thickness $\rho_s d$, by a temperature-independent amount $\rho_s l_h=1.47\times10^{-8}$ g/cm^2. This quantity is relatively insensitive to the value of the unknown parameter M, varying by no more than about 10% as M is varied from zero to infinity. That the reduction in areal superfluid density is temperature independent is a consequence of the fact that the healing length diverges at the same rate that the superfluid density approaches zero at the transition temperature. We use the *measured* bulk superfluid density in the calculation so as to extend the range of validity of the calculation to temperatures relatively far from the transition, in the spirit of Ginzburg and Sobyanin.

The Kosterlitz-Thouless recursion relations can be written in terms of the parameters K, proportional to the scale-dependent areal superfluid density, and y^2, the vortex-pair excitation probability:

$$\begin{aligned} K^{-1}(l)&=K_0^{-1}+4\pi^3\int_0^l y^2(l')dl' \ , \\ y^2(l)&=y_0^2\exp\left[4l-2\pi\int_0^l K(l')dl'\right] \ , \end{aligned} \tag{2.6}$$

where

$$l=\ln(r/r_0) \ . \tag{2.7}$$

r_0 is the vortex core radius,

$$K^{-1}(l)=\tilde{\varepsilon}(l)/K_0 \ , \tag{2.8}$$

where K_0 is defined in terms of the bare superfluid density as $(\hbar/m)^2\sigma_s^0/k_BT$, $\tilde{\varepsilon}(l)$ represents the attenuating effect of smaller pairs on the interaction between the respective members of larger pairs with separation e^l, and

$$y_0^2=\exp(-E_p/k_BT) \ , \tag{2.9}$$

where $E_p(T)$ is the temperature-dependent energy associated with the primordial vortex pair, clearly proportional to σ_s^0 and dependent on the assumption made as to its structure. We assume that the cores of the vortices in the primordial pair are separated by twice the core radius and that the core energy is as given by the "dynamical scaling" approach of Kawatra and Pathria.[27] This latter is a straightforward adaptation of the theory of Ginzburg and Pitaevskii.[24] These considerations yield the relation $E_p/k_BT=6.72K_0$.

The observed superfluid density σ_s in this theory is

$$\sigma_s(T)=\sigma_s^0(T)/\tilde{\epsilon}(l=\infty) . \tag{2.10}$$

The vortex-excitation probability y^2 is related to the density of pairs per unit area of separation $\delta n(r)$ by

$$y^2(l=0,T)=y_0^2(T) , \tag{2.11}$$

$$K(l=0,T)=K_0(T) . \tag{2.12}$$

The static transition temperature $T_{\rm KT}$ is defined as the largest temperature for which

$$\lim_{l\to\infty} y^2(l,T_{\rm KT})=0 \tag{2.13}$$

or equivalently by

$$\lim_{l\to\infty} \tilde{\epsilon}(l,T_{\rm KT})=\pi K_0/2 , \tag{2.14}$$

and is the temperature at which the pairs of infinite separation unbind. Above $T_{\rm KT}$ both $\tilde{\epsilon}$ and y^2 become large, indicating that σ_s^0 is being renormalized to zero and that very large pairs are becoming significantly probable. Note that Eq. (2.14) implies that

$$\sigma_s(T_{\rm KT})=\frac{2k_B m^2}{\pi\hbar^2}T_{\rm KT} . \tag{2.15}$$

This is one of the principal results of the static theory. Equation (2.15) predicts a universal jump in superfluid density at the static transition temperature.

The effect of finite frequency is simply to truncate iteration of the recursion relations, Eqs. (2.6), at a scale l_ω, the vortex diffusion length. l_ω is given by

$$l_\omega=\frac{1}{2}\ln\left[\frac{14D}{\omega r_0^2}\right] , \tag{2.16}$$

where ω is the angular frequency of the substrate oscillations and D is the vortex diffusivity. Although D is a temperature-dependent quantity,[27] and indeed appears to diverge at the transition, its influence on the transition temperature is relatively weak, and we assume a constant value of order $\hbar/m$. Vortex pairs larger than this scale do not have time to equilibrate with the imposed velocity field and therefore do not participate in screening. This results in a somewhat enhanced superfluid density, a broadening of the phase transition which is shifted to slightly higher temperature, and a dissipation peak at the transition.

We have assumed until now that infinitesimal external fields are used to probe the vortex plasma. In practice this assumption is easily violated, thus requiring an analysis of nonlinear finite amplitude effects. We follow the approach outlined by Adams and Glaberson,[28] in which the recursion relations are modified by the inclusion of a Bessel function term. In addition, a new length scale associated with the imposed velocity field is introduced and it is this scale at which the iteration procedure is truncated when it is smaller than the vortex diffusion scale. Finite amplitude effects give rise to a broadening of the transition, an increase of the superfluid dissipation in the vicinity of the transition and a shift of the transition to larger film thickness.

As pointed out by Agnolet, McQueeney, and Reppy,[18] measured quantities in the vicinity of the Kosterlitz-Thouless transition should show a universal scaling form

$$\begin{aligned}\frac{2\Delta P/P}{\sigma_s^0(T)}&=G_1[X,l_\omega,F,\sigma_s^0(T_c)/T_c] ,\\ \frac{\Delta Q^{-1}}{\sigma_s^0(T)}&=G_2[X,l_\omega,F,\sigma_s^0(T_c)/T_c] ,\end{aligned} \tag{2.17}$$

where $x=(T/T_c)\sigma_s^0(T_c)/\sigma_s^0(T)$, and F is the prefactor in the expression for the free vortex density. Near T_c they obtained the approximate scaling relation

$$\begin{aligned}\frac{2\Delta P/P}{T_{\rm peak}}&=H_1[T/T_{\rm peak},l_\omega,F,\sigma_s^0(T_c)/T_c] ,\\ \frac{\Delta Q^{-1}}{T_{\rm peak}}&=H_2[T/T_{\rm peak},l_\omega,F,\sigma_s^0(T_c)/T_c] .\end{aligned} \tag{2.18}$$

These relations are appropriate for experiments in which the film thickness is fixed and the transition is scanned by varying the temperature. Our transition scans were not done at fixed layer thickness but rather at a fixed temperature. The equivalent scaling relation near the transition suggests universal behavior in plots of f/T_c and Q^{-1}/T_c as a function of $(d-d_c)\rho_s/T_c$, where d is the film thickness, d_c is the film thickness at transition, and ρ_s is the bulk superfluid density. This universality is indeed confirmed in detailed numerical calculations, even when including effects of finite amplitude and of finite-size scaling, but breaks down somewhat when account is taken of the temperature dependence of the vortex core radius.

The simplest approach to incorporating the effects of the dead layer is to assume that the superfluid wave function is zero at the dead layer–superfluid interface and heals in the manner described above. The dead layer would not then contribute to the vortex-pair energy. A slight complication arises from the introduction of a spatially varying healing length associated with the pressure gradient in the film outside of the dead layer. For all practical purposes, the net result of these considerations is simply to add a fixed amount—estimated to be approximately 6 Å—to the critical film thickness. As indicated above, one could also argue that this approach involves "double counting" and that the wave function in fact penetrates into the dead layer.

III. EXPERIMENTAL METHOD

A. Quartz-crystal microbalance method

The quartz-crystal microbalance technique for the study of superfluidity involves the work of Chester, Yang, and Stephens.[20,21] Their method consisted of monitoring the frequency of the crystal oscillations, while continuously changing the thickness of a helium film adsorbed on its surface. Because the normal component of the liquid film adsorbed contributes to the mass loading of the crystal, the resonant frequency of the oscillator is lowered.

The superfluid fraction can be deduced by subtracting the normal component from the total mass per unit area adsorbed onto the surface of the crystal.

In the present experiment we have used a high-Q crystal[29] for simultaneous measurement of the superfluid density and dissipation in the transition region. Two separate crystals with different resonant frequencies were used to study the dynamic characteristic of the Kosterlitz-Thouless transition. Two different series of experiments were undertaken. In the first, use was made of a single SC-cut 5-MHz crystal, oscillating in the fifth harmonic thickness shear mode. The crystal thickness was 0.16 cm thick having gold evaporated electrodes on 30% of its surface area. The Q of the crystal was exceptionally high, 2×10^6 at room temperature and 5×10^6 at 4.2 K. The driving circuit was a standard Colpitz oscillator, where the feedback conditions correspond to the minimum impedance of the crystal. This circuit requires relatively high amplitudes to maintain stable oscillations. The change of the amplitude, or alternatively of the Q, of the oscillations was measured simultaneously with the frequency. Since there is relatively little damping in the quartz crystal, the amplitude of the oscillations is sensitive to the internal dissipation of the superfluid at the transition. With our experimental apparatus, frequency changes of one part in 5×10^9, and of one part in 10^6 in the amplitude could be observed.

In the second series of experiments, two crystals resonating at 5 and 10 MHz were mounted at the same height in the cell. Both crystals were AT-cut, operating in the resonant thickness shear mode in first harmonic. Working in the basic harmonic reduced the thickness of the crystals to 0.03 and 0.015 cm for 5 and 10 MHz, respectively, thus improving their mass sensitivity. Silver electrodes covered about 40% of the surface area. The Q factor of the crystals ranged from 1.5×10^5 at room temperature to 2.5×10^5 at 4.2 K. Each of the crystals was driven by a separate circuit, designed for their capability of driving the crystals at relatively low amplitudes that could be regulated between 0.8 and 4 mV.

B. Response of the piezoelectric crystal

Each of the principal surfaces of the crystal vibrates in the plane of the surface and is subject to the force exerted by the film and vapor present. It is convenient to describe this force in terms of the acoustic impedance $Z(\omega)$. $Z(\omega)$ can be written as the sum of the reactive part $X(\omega)$, which reflects the inertia, and the resistive part $R(\omega)$, which is associated with dissipation:

$$Z(\omega)=R(\omega)-iX(\omega)\ . \tag{3.1}$$

If both surfaces of the crystal are subject to the same impedance we obtain the change in frequency and dissipation

$$\Delta\omega=\frac{4X(\omega)}{\rho_q d_q}\ ,\qquad \Delta\left[\frac{1}{Q}\right]=\frac{4R(\omega)}{\rho_q d_q}\ , \tag{3.2}$$

where ρ_q and d_q are the density and the thickness of the quartz crystal. The transverse-acoustic impedance of the liquid film of thickness d, including the effect of the vapor, is given by[30]

$$Z(\omega)=(1-i)\left[\eta_l\rho_l\frac{\omega}{2}\right]^{1/2}\tanh\left[\Psi+(1-i)\frac{d}{\delta}\right]\ , \tag{3.3}$$

where ρ_l is the density and η_l is the viscosity of the liquid film, δ is the viscous penetration depth given by $\delta=(2\eta_l/\rho_l\omega)^{1/2}$, and Ψ is defined by the relation

$$\tanh(\Psi)=\left[\frac{\eta_v\rho_v}{\eta_l\rho_l}\right]^{1/2}\ , \tag{3.4}$$

ρ_v and η_v being the density and viscosity of the vapor. Even for the higher frequency, 10 MHz, $\delta=245$ Å is much larger than the thickness of the thickest film. We can then approximate the impedance to obtain

$$Z(\omega)=(1-i)\left[\eta_v\rho_v\frac{\omega}{2}\right]^{1/2}-i\rho_l d\omega\ . \tag{3.5}$$

For the frequency shift we obtain

$$\Delta\omega=-2\left[\frac{\rho_l d}{\rho_q d_q}\right]\omega-2\left[\frac{\eta_v\rho_v\omega}{2\rho_q d_q}\right]^{1/2}\ . \tag{3.6}$$

The first term in Eq. (3.6) is the familiar expression for a microbalance with mass loading and the second is the contribution of the vapor. If the film is thin, this contribution cannot be neglected.

In the case of liquid He only the normal component contributes to the frequency change, hence we can replace $\rho_l d$ with $\rho_n d=\rho_{\mathrm{He}}d-\sigma_s$. ρ_{He} is the bulk liquid-helium density, where we ignore effects of the van der Waals-induced pressure gradient in the film. For our crystals the frequency shift associated with a single atomic layer of helium (≈3.6 Å) is $\Delta f=-0.148$ Hz for the SC-cut 5-MHz crystal, $\Delta f=-0.8$ Hz for the AT-cut 5-MHz crystal, and $\Delta f=-3.2$ Hz for the AT-cut 10-MHz crystal. Our experimental sensitivity of 0.001 Hz allows for observing changes smaller than 1/100 of an atomic layer.

In order to extract useful quantitative information concerning superfluid dissipation from our data, it is necessary to relate the Q factor of the oscillator to the amplitude of its oscillations which depends on the value of a bias voltage in the circuit. We decided that it would not be particularly useful to attempt this by means of a detailed analysis of the electronic circuit because of the uncertainty of various component parameters. We chose, instead, a calibration procedure as follows: Near resonance, the piezoelectric crystal can be modeled by the equivalent circuit shown in Fig. 1, where $Q\equiv\omega L/R$. The calibration was carried out in two stages: In the first, the cell was evacuated, the temperature was stabilized and the feedback circuit was replaced by an ac current source. We performed a series of measurements of the amplitude as a function of frequency at different gas pressures inside the cell as shown in Fig. 2. For each scan the parameters of the equivalent circuit were fitted

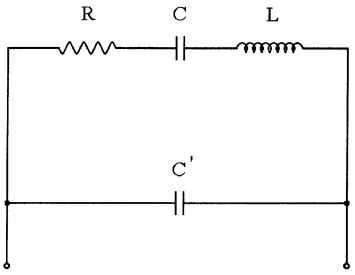

FIG. 1. Equivalent circuit for the piezoelectric crystal. For the unloaded crystal, the values of the components are $L=21$ H, $R=225$ O Ω, $C=4.8\times10^{-8}$ F, and $C'=1.53\times10^{-10}$ F.

and Q was determined as a function of the pressure P. In the second stage the current source was replaced by the feedback circuit and a series of measurements of the frequency of oscillation f, and of the amplitude A as a function of pressure, for the different bias voltages of the circuit, was carried out. From the first stage we obtained $1/Q$ as a function of P and from the second stage we obtained A as a function of P for each value of the bias voltage. By combining the results we obtained $1/Q$ as a function of A.

C. Film thickness

Helium contained in the experimental cell adsorbs onto the crystal surface by means of the van der Waals interaction. The film thickness d can be determined by equating the van der Waals potential $U(d)$ to the change in chemical potential associated with bringing an atom from a condition of saturated pressure P_0 to that at lower pressure P, which for an ideal gas is given by

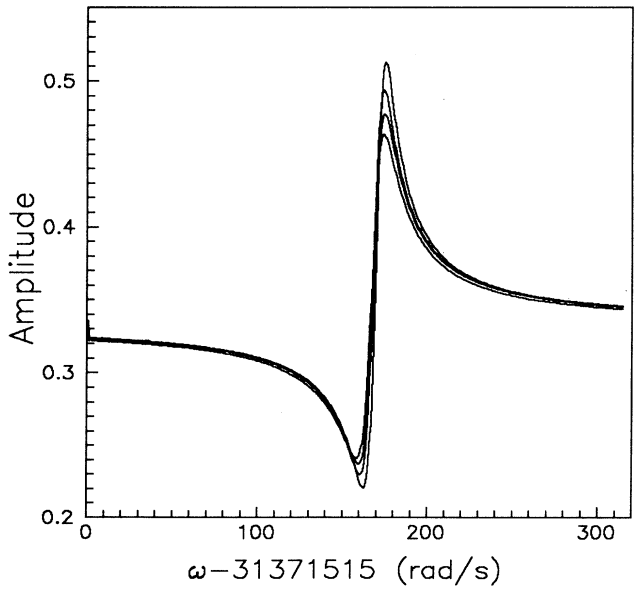

FIG. 2. Amplitude of the voltage on the crystal as a function of frequency for various gas pressures. This quantity is proportional to the magnitude of the crystal impedance.

$$U(d)=\Delta\mu=-k_B T\ln(P/P_0)\ . \tag{3.7}$$

A detailed description of the macroscopic forces between a solid body and the thin film adsorbed on it was given by Dzyaloshinsky, Lifshitz, and Pitaevskii[31] (DLP). Treating this problem as a special case of their general theory of the van der Waals forces, the following expression for $U(d)$ was derived

$$U(d)=\alpha'(d)d^{-3}\ . \tag{3.8}$$

The equations used to calculate the coefficient $\alpha'(d)$ require information about the dielectric properties of the substrate and the adsorbate. Nevertheless a general dependence of $\alpha'(d)$ on thickness, following from these equations, is that $\alpha'(d)$ decreases with d from the $\alpha'(d=0)$ value to an asymptotic d^{-1} behavior in the very thick-film limit due to retardation effects. Analytical and numerical calculations of Cheng and Cole[32] made it apparent that these effects can be neglected when $d\ll100$ Å, while for $d\sim200$ Å the effect of retardation is to reduce the thickness by 20% relative to that calculated with $\alpha'(d=0)$. Since in the present experiment d is always smaller than 100 Å the simplified form of $U(d)$ with $\alpha'(d=0)$ is utilized. Defining $\alpha=\alpha'(0)/k_B$, the thickness is given by

$$d=\left[\frac{-\alpha}{T\ln(P/P_0)}\right]^{1/3}\ . \tag{3.9}$$

The suitability of DLP theory for predicting film thickness was experimentally verified by Sabisky and Anderson.[33] Thicknesses of planar helium films on alkaline-earth fluoride substrates, measured using an acoustic interferometry technique, was found to be remarkably consistent with that predicted by the DLP theory. However, it appears that for the substrates of interest in the present work there is disagreement between the empirical values of α and those obtained using theoretical calculation. Reported values are listed in Table I.

To determine film thickness in our experiments we use the empirical values listed in Table I. Because these appear to be very close to each other, and since d only weakly depends on α, we neglect the effect of the inhomogeneity introduced by the evaporated electrode on the crystals. We use $\alpha=42$ K layers[3] for the gold-plated electrode of the SC-cut crystal and 40 K layers[3] for the silver electrode crystals.

D. Procedure

Our experimental system consists of an experimental cell containing the crystals within a pumped outer helium bath. The crystal cell is provided with two $\frac{1}{4}$ inch open-

TABLE I. Interaction coefficients. Units are K layers (Ref. 3).

Substrate	Empirical	Theoretical
Quartz	39 (Ref. 21)	25.3
Silver	40 (Ref. 34)	75.86 (Ref. 35)
Gold	42 (Ref. 36)	66.45 (Ref. 32)

ings, for reasons discussed below.

The experimental procedure is begun by regulating the outer bath to a definite temperature. After the evacuated cell has equilibrated with the outer bath, the pressure P in the experimental cell is swept isothermally by a continuous addition of gas up to the saturation pressure P_0. After the helium is well saturated the procedure is reversed: beginning with saturated liquid, the gas is slowly removed to the lowest pressure of the sweep. Although sweeping to low pressure is preferred because of a better thermal coupling of the crystals to the bath via the gas in the chamber, the thin-film limit cannot be achieved this way owing to the low density of the gas at the corresponding low pressure. Whenever measurements in very thin films were taken, the system was warmed before the crystal cell was evacuated.

While control of the amount of gas in the cell is carried out through one of its openings, the second opening serves to monitor the pressure throughout the sweep. Because the thickness of the film depends strongly on P, even small flow impedance within the access tube would result in an incorrect determination of the film thickness were only one tube utilized. In the manner described here a direct measurement of P_0 is made whenever the helium achieves saturation in the experimental cell. Thus, even if the temperature assumed for a given sweep deviates slightly from the actual temperature, this will affect the thickness only through the explicit temperature dependence in the denominator of Eq. (3.9) but not through the much stronger dependence on P_0.

IV. EXPERIMENTAL RESULTS

The different devices were controlled by a computer and data were gathered as a function of the pressure inside the cell. Near saturation, the pressure difference between the cell and the helium reservoir was monitored. Typical results are shown in Figs. 3 and 4. One can

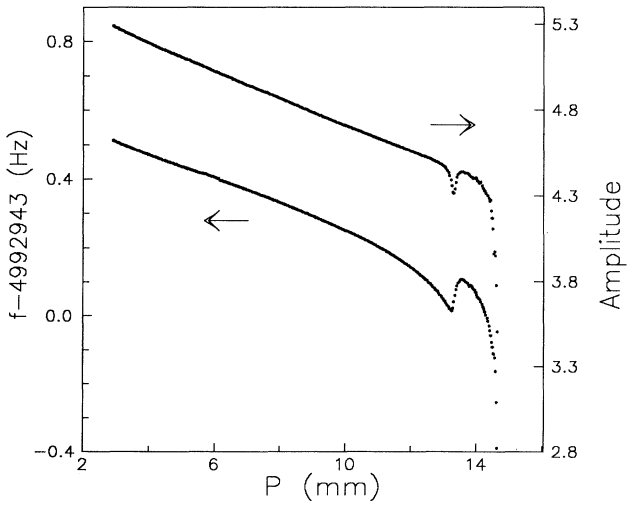

FIG. 3. Typical pressure scan at a fixed temperature of 1.85 K, corresponding to a saturated vapor pressure of 14.7 mm. The superfluid transition is associated with the rapid rise in frequency and the amplitude dip at about 13 mm pressure.

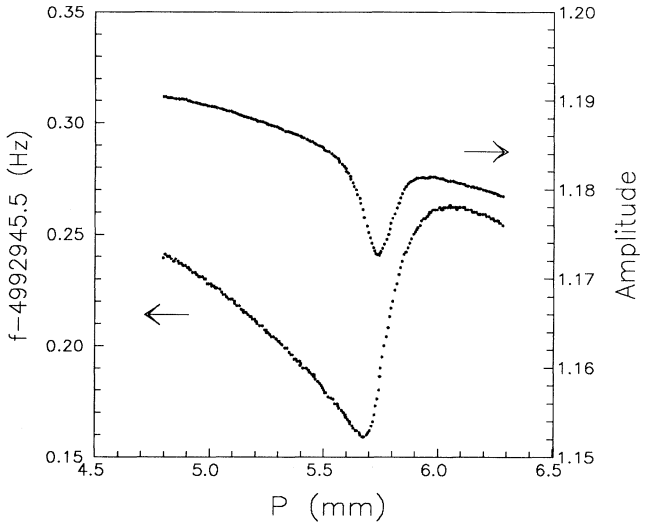

FIG. 4. Pressure scan in the vicinity of the superfluid transition at $T=1.66$ K.

clearly see the decrease in amplitude caused by the excess dissipation in the vicinity of the transition and the sharp increase in frequency. There is no sharp discontinuity like that which appears in the static theory, but rather a continuous rise. As we shall see, the rounding of the transition is consistent with a combination of effects associated with finite amplitudes and thickness inhomogeneity.

In all of our analysis we assume that the film thickness is determined by the vapor pressure, as described earlier. We are not completely comfortable with this assumption because it is not entirely consistent with the observed frequency response of the crystal as the pressure is varied in the normal-fluid regime. Plotting a series of isotherms as a function of a quantity proportional to the film thickness, calculated in this manner, yields the curves shown in Fig. 5. Contrary to our expectations, the background

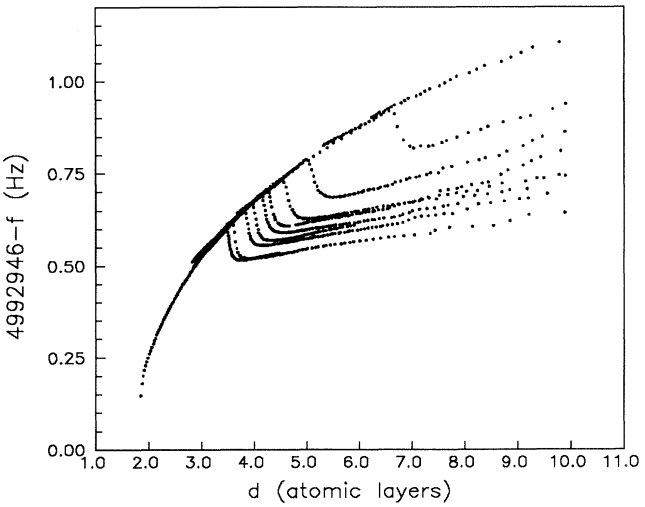

FIG. 5. Frequency as a function of film thickness for temperatures ranging from 1.38 to 2.12 K.

curve is far from linear in shape. The observed discrepancy is much larger than can be explained by effects of gas pressure, nonideal gas behavior, dead layer effects, or retardation. At the largest film thickness shown in the figure, about 50 Å, retardation effects give rise to less than a 5% shift. We have no explanation to offer for this discrepancy, but we nevertheless believe that our thickness determination is correct. This belief is confirmed by our observation that despite the lack of complete reproducibility of the frequency versus pressure plots, the critical pressure, at a given temperature, always reproduces exactly.

A. Frequency measurements

As gas is added to the cell, the thickness of the adsorbed film increases and the crystal frequency decreases. As the critical thickness is exceeded, some fraction of the adsorbed film decouples from the substrate and the frequency increases almost discontinuously. As still more gas is added, the film continues to grow in thickness and the frequency decreases, but at a somewhat slower rate. In order to extract the areal superfluid density, the frequency is subtracted from an extrapolation of the pretransition behavior. In Fig. 6 we show the superfluid density as a function of film thickness. The vertical axis is the dimensionless quantity $(\sigma_s/T_c)/\beta$, where $\beta=3.5\times10^{-9}$ g/cm^2 K is the Kosterlitz-Thouless parameter and the horizontal axis is the dimensionless quantity $[(d-d_c)(\rho_s/T_c)]/\beta$. As expected from our discussion of scaling behavior, the data covering a wide range of temperatures and transition thicknesses coalesce reasonably onto a common curve. Numerical calculation yields the curves shown in Fig. 7, covering the same range of temperatures, where the calculated superfluid densities have been reduced by 35%. It is not at all surprising that the calculated superfluid densities overestimate the observed values by a factor of order unity, since any deviation of the substrate from flatness on an atomic scale will give rise to some fraction of the superfluid being dragged along with the substrate and therefore to a reduction of the effective superfluid fraction. Perhaps the small scatter in the data far from d_c reflects a small thickness dependence of this parameter. It is clear that reasonable consistency between the measured and calculated superfluid densities exists and that the suggested scaling relations work reasonably well.

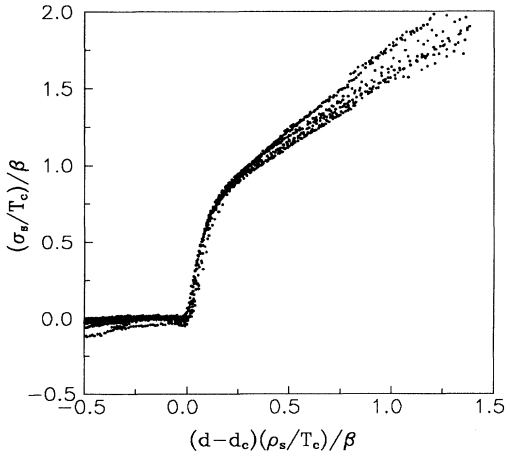

FIG. 6. Dimensionless areal superfluid density as a function of dimensionless film thickness in the vicinity of the transition. The curves represent data for temperatures ranging from 1.38 to 1.96 K.

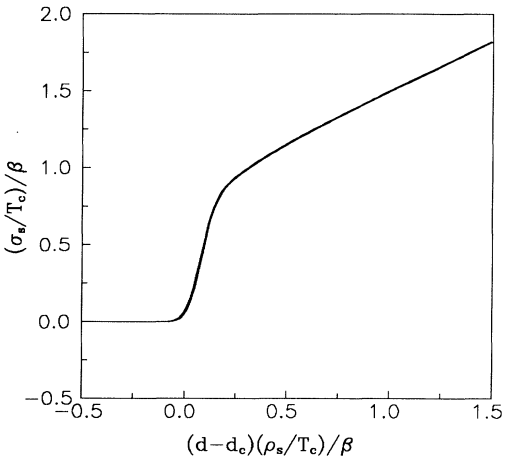

FIG. 7. Results of numerical calculation of the superfluid density for two temperatures at the extremes of the data shown in Fig. 6.

B. Amplitude measurements

Measurements of the oscillation amplitudes were used to extract superfluid dissipation using the calibration procedure described above. $1/Q$ versus film thickness data, covering the full range of temperatures studied, is shown in Fig. 8. Plotting the data as suggested by the scaling relations yields the curves in Fig. 9. The scaling relations clearly work well.

Straightforward numerical calculation yields dissipation peaks somewhat smaller than observed and, more

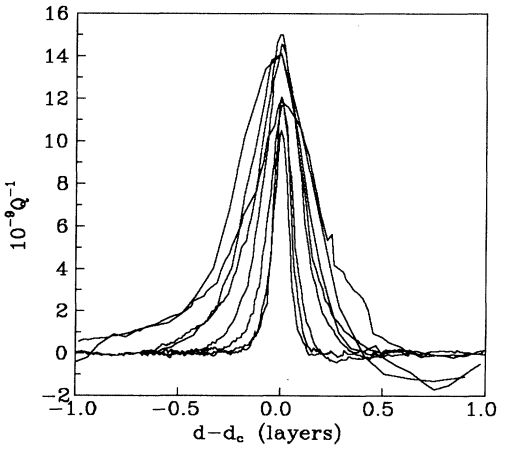

FIG. 8. Inverse Q as a function of film thickness for temperatures ranging from 1.38 to 1.96 K.

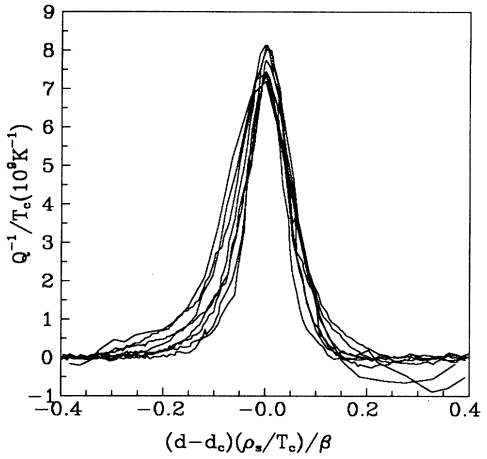

FIG. 9. Q^{-1}/T as a function of dimensionless film thickness for the data shown in Fig. 8.

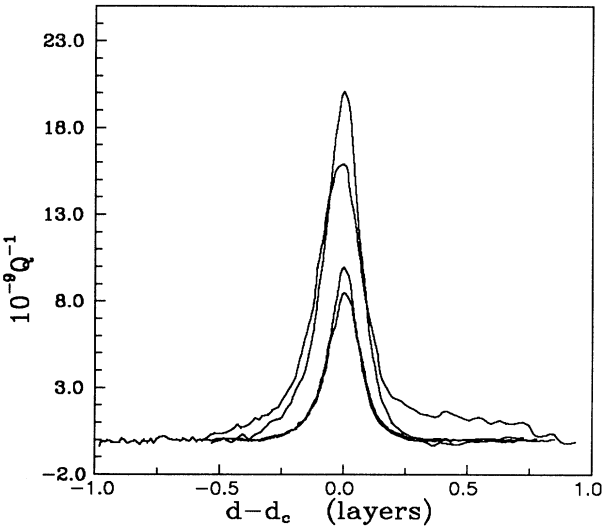

FIG. 11. Inverse Q as a function of the film thickness for various oscillation amplitudes at a fixed temperature of 1.51 K.

significantly, having an integrated area more than a factor of 3 smaller. It would seem that two separate effects are involved. Film thickness inhomogeneity, perhaps arising from inhomogeneity of the van der Waal's constant, would broaden the peak but not change its area. Finite amplitude nonlinear effects, on the other hand, would both broaden and increase the height of the dissipation peak. A direct independent determination of these quantities proved impossible. Fits to the data yield a convoluting thickness inhomogeneity having a half width of 3.5% and a substrate oscillation amplitude of approximately 40 Å. Figure 10 shows calculated dissipation peaks for two temperatures spanning those of the data which incorporate both of these factors. These factors were also incorporated into the numerical results shown in Fig. 7 for the superfluid density.

We measured a number of isotherms at the same temperature ($T=1.66$ K) but at different circuit bias voltages and therefore different amplitudes. The results from these measurements are shown in Figs. 11 where the nonlinear increase of dissipation with amplitude can be clearly seen. The critical film thickness increases with increasing amplitude, as shown in Fig. 12. Heating of the crystal at higher amplitudes could be responsible for the observed shifts of transition pressure. Numerical calculation indicates that these shifts are at least a factor of 5 larger than can be explained solely on the basis of nonlinearity.

In addition to the monotonic decrease in amplitude with increasing pressure and the dip at the transition, a number of new phenomena appeared for relatively thick films. Even before the phase transition, we observed accurately reproducible oscillations in the amplitude. Close to the saturated vapor pressure the monotonic decrease in amplitude ceases and the amplitude increases. Examples of these phenomena are shown in Fig. 13. As the os-

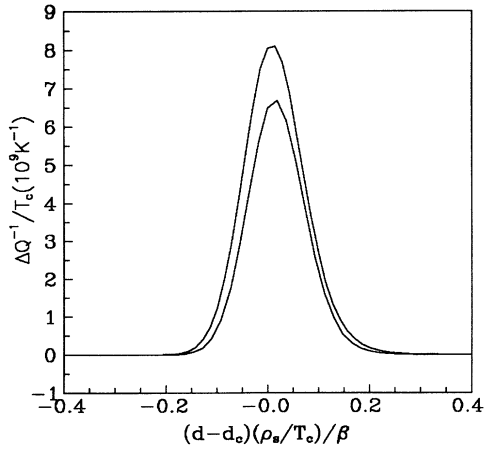

FIG 10. Numerical calculation of inverse Q for two temperatures at the extremes of the data shown in Fig. 9.

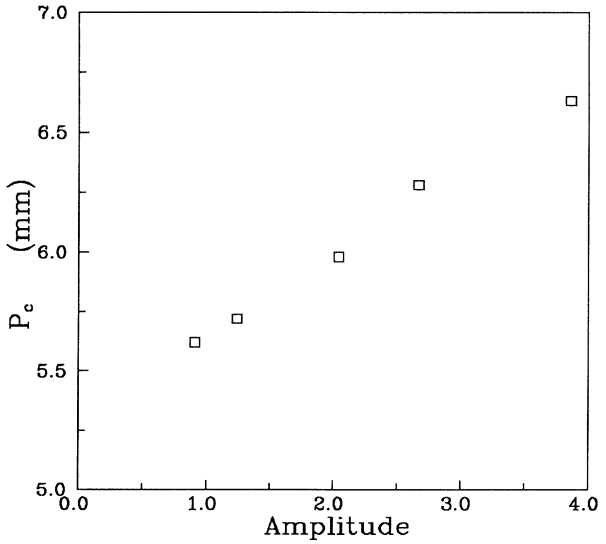

FIG. 12. Shift of the critical vapor pressure as a function of oscillation amplitude at a fixed temperature of 1.51 K.

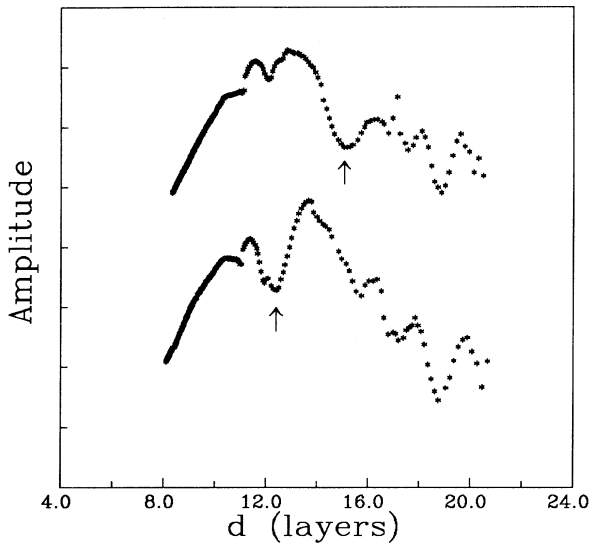

FIG. 13. Amplitude as a function of film thickness. The upper curve corresponds to a temperature $T=2.1$ K and the lower curve to a temperature 20 mK lower. The arrows indicate the locations of the superfluid transitions.

cillator drive was decreased, these phenomena appeared at higher temperatures and thicker layers. In the figure we show two runs at slightly different temperatures, and therefore different critical thicknesses, but for which the amplitude oscillations appear fixed. It would therefore appear that these phenomena are unrelated to superfluid transition effects, but we offer no explanation for them.

C. Critical film thickness

Calculations of the critical film thickness as a function of critical temperature are shown in Figs. 14 and 15, with and without the dead layer, and are compared with our experimental data and that of Yu, Finotello, and Gasparini.[37] The calculations were carried out by directly iterating the recursion relations, Eq. (2.6), from the starting conditions and parameters described in Sec. II B, until the point where the superfluid density is reduced by an order of magnitude. It is clearly difficult to obtain a precise conclusion regarding the dead layer, but overall consistency with the calculations is evident. We point out that our approach, in starting the Kosterlitz-Thouless iteration procedure from a state in which finite-size scaling has already significantly reduced the bare superfluid density, is crucial to the approximate quantitative agreement between experiment and calculation. Some discrepancy remains between the theoretical curves and our measured data, particularly for the thinner films, possibly associated with the breakdown of the Ginzburg-Sobyanin expansion to temperatures far from the bulk transition. Ignoring finite-size scaling effects reduces the calculated critical film thicknesses by more than a factor of 3 and substantially increases this discrepancy.

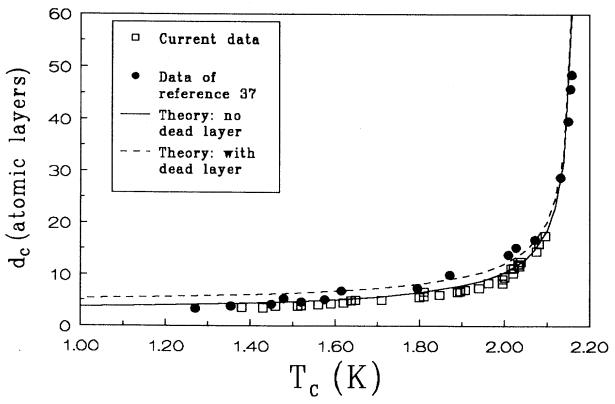

FIG. 14. A linear plot of critical film thickness as a function of temperature. The lines are the result of the numerical calculation with (dashed) and without (solid) including the effect of a dead layer.

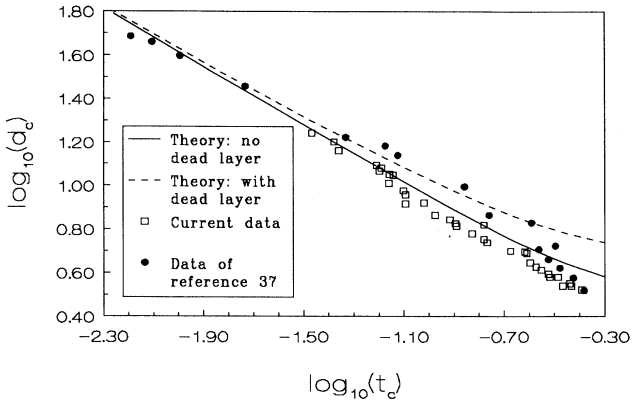

FIG. 15. A log-log plot of critical film thickness as a function of reduced temperature ($t_c=1-T_c/T_\lambda$). The lines are the result of the numerical calculation with (dashed) and without (solid) including the effect of a dead layer.

D. Dynamical effects

An experiment was undertaken to investigate the effect of finite frequencies on the Kosterlitz-Thouless transition. As pointed out earlier, increasing the frequency of the probe ought to give rise to a shift of the transition thickness to smaller values. This is true, however, only when the truncation of the Kosterlitz-Thouless iteration procedure is determined by the vortex diffusion length scale and not by the finite velocity length scale that gives rise to nonlinear effects. In addition, the transition thickness depends on oscillation amplitude so long as nonlinear effects are present. Care was therefore taken to insure relatively small amplitudes, as discussed in Sec. II B. We were indeed successful in operating the AT-cut crystals at oscillation levels almost two orders of magnitude smaller and verified that transition thickness and width in this new system were insensitive to changes in amplitude. The price that we had to pay for using these new crystals was that the inhomogeneity induced transition width was substantially larger, presumably because of the different surface treatment, and, in addition, we did not have sufficient amplitude resolution to extract dissipation information.

Two crystals, one operating at 5 MHz and the other at 10 MHz were placed in the experimental cell and operated simultaneously. In order to insure that the chemical potential was equal at the two crystals, they were mounted at the same height in the cell. Interchanging the crystals had no effect on the results. In this manner, we were able to map out the transition at two frequencies under almost identical circumstances. The results of a typical transition scan, at $T=1.51$ K, are shown in Fig. 16. The shift of the higher frequency transition to smaller film thickness is evident. Numerical calculation yields shifts of the same magnitude for a vortex diffusivity equal to $0.04\hbar/m$. Since little, *a priori*, is known about this quantity, these results are deemed satisfactory.

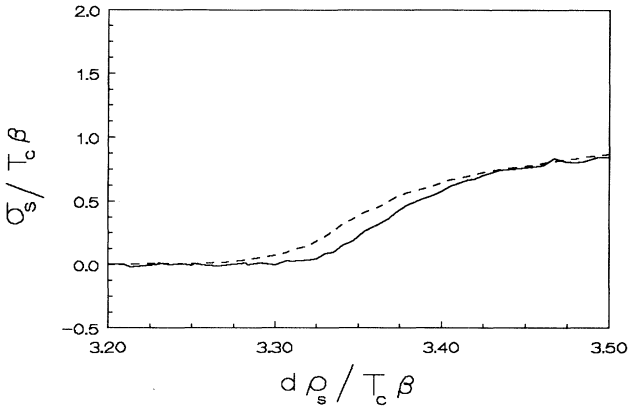

FIG. 16. Transition scans at two different frequencies, 5 MHz (solid line) and 10 MHz (dashed line), at a temperature $T=1.51$ K.

V. CONCLUSIONS

We have been able to extend the use of the quartz microbalance as an effective tool for investigating fundamental issues associated with the superfluid transition in two-dimensional layers of liquid helium. The results are found consistent with a detailed numerical calculation in which the Kosterlitz-Thouless recursion relations are iterated from unrenormalized, or bare, starting conditions determined by a particular expression of finite-size scaling theory using reasonable values for all the relevant parameters. Consistency is found with respect to the shape of the transition in both superfluid density and dissipation, the dependence of critical layer thickness on temperature, and shifts of critical thickness with oscillator frequency. Uncertainty remains as to the exact values of a number of parameters used and our results cannot be seen as an absolute proof that the approach we have taken is the correct one. We emphasize, however, that our intention is to present a consistent picture of the transition, and in this we believe that we have succeeded.

ACKNOWLEDGMENTS

We acknowledge very useful discussions with F. Gasparini. This research was supported by Grant No. 89-43 from the United States–Israel Binational Science Foundation and Grant No. 140/90-1 from the Israel Academy of Sciences and Humanities. R.B. received financial support from the Leon David Asseo Foundation.

*Present address: Department of Nuclear Physics, Weizmann Institute of Science, Rehovot, Israel.

[1]D. R. Nelson, *Phase Transitions* (Academic, London, 1983), Vol. 7.

[2]J. M. Kosterlitz and D. J. Thouless, J. Phys. C **6**, 1181 (1973).

[3]D. R. Nelson and J. M. Kosterlitz, Phys. Rev. Lett. **39**, 1201 (1977).

[4]V. Ambegaokar, B. I. Halperin, D. R. Nelson, and E. D. Siggia, Phys. Rev. Lett. **40**, 783 (1978).

[5]V. Ambegaokar and S. Teitel, Phys. Rev. B **19**, 1667 (1979).

[6]F. M. Gasparini and I. Rhee, in *Progress in Low Temperature Physics XIII,* edited by D. F. Brewer (North-Holland, Amsterdam, 1992).

[7]E. Long and L. Meyer, Phys. Rev. **79**, 1031 (1950); **85**, 1030 (1952).

[8]P. C. Hohenberg, Phys. Rev. **158**, 383 (1967).

[9]R. Bowers, D. F. Brewer, and K. Mendelssohn, Philos. Mag. **42**, 1445 (1951).

[10]E. Long and L. Meyer, Phys. Rev. **98**, 1616 (1955).

[11]D. F. Brewer and K. Mendelssohn, Proc. R. Soc. Ser. A **260**, 1 (1961).

[12]R. P. Henkel, E. N. Smith, and J. D. Reppy, Phys. Rev. Lett. **23**, 1276 (1969).

[13]C. W. Everitt, K. R. Atkins, and A. Denenstein, Phys. Rev. **136**, A1494 (1964).

[14]I. Rudnick, R. S. Kagiwada, J. C. Fraser, and E. Guyon, Phys. Rev. Lett. **20**, 430 (1968).

[15]I. Rudnick, Phys. Rev. Lett. **40**, 1454 (1978).

[16]E. L. Andronikashvili, Zh. Teor. Fiz. **16**, 780 (1946).

[17]D. J. Bishop and J. D. Reppy, Phys. Rev. Lett. **40**, 1727 (1978).

[18]G. Agnolet, D. F. McQueeney, and J. D. Reppy, Phys. Rev. B **39**, 8934 (1989).

[19]K. Shirahama, M. Kubota, and S. Ogawa, in Proceedings of the 19th International Conference on Low Temperature Physics, edited by D. S. Betts, M. Durieux, and G. H. Lander [Physica B **165 & 166**, 545 (1990)]; K. Shirahama, M. Kubota, S. Ogawa, N. Wada, and T. Watanabe, Phys. Rev. Lett. **64**, 1541 (1990).

[20]M. Chester, L. C. Yang, and J. B. Stephens, Phys. Rev. Lett. **29**, 211 (1972).

[21]M. Chester and L. C. Yang, Phys. Rev. Lett. **31**, 1377 (1973).

[22]J. A. Herb and J. G. Dash, Phys. Rev. Lett. **29**, 846 (1972).

[23]V. L. Ginzburg and A. A. Sobyanin, Usp. Fiz. Nauk **120**, 153 (1976) [Sov. Phys. Usp. **19**, 773 (1976)]; J. Low Temp. Phys. **49**, 507 (1982).

[24]V. L. Ginzburg and L. P. Pitaevskii, Zh. Eksp. Teor. Fiz. **7**, 1240 (1958) [Sov. Phys. JETP **34**, 858 (1958)].

[25]See, e.g., T. Oestereich and H. Stenschke, Phys. Rev. B **16**, 1966 (1977).

[26]See, e.g., P. Sindzingre, M. L. Klein, and D. M. Ceperley, Phys. Rev. Lett. **63**, 1601 (1989).

[27]M. P. Kawatra and R. K. Pathria, Phys. Rev. **151**, 132 (1966).
[28]P. W. Adams and W. I. Glaberson, Phys. Rev. B **35**, 4633 (1987).
[29]The crystals were obtained from TFL Ltd., P.O.B. 1792, Holon, Israel.
[30]D. S. Spencer, M. J. Lea, and P. Fozooni, Phys. Rev. Lett. **109A**, 295 (1985).
[31]I. E. Dzyaloshinskii, E. M. Lifshitz, and L. P. Pitaevskii, Adv. Phys. **10**, 165 (1961).
[32]E. Cheng and M. W. Cole, Phys. Rev. B **38**, 987 (1988).
[33]E. S. Sabisky and C. H. Anderson, Phys. Rev. A **7**, 790 (1973).
[34]A. D. Migone, J. Krim, and J. Dash, Phys. Rev. B **31**, 7643 (1985).
[35]S. Rauber, J. R. Klein, M. W. Cole, and L. W. Bruch, Surf. Sci. **123**, 173 (1983).
[36]M. J. Lea, D. S. Spencer, and P. Fozooni, Phys. Rev. B **35**, 6665 (1987).
[37]Y. Y. Yu, D. Finotello, and F. M. Gasparini, Phys. Rev. B **39**, 6519 (1989). Note that the theoretical curves in this paper ignore Kosterlitz-Thouless renormalization.